

1 A comparison of gap-filling algorithms for eddy covariance 2 fluxes and their drivers

3

4 Atbin Mahabbati¹, Jason Beringer¹, Matthias Leopold¹, Ian McHugh², James Cleverly³, Peter Isaac⁴,
5 Azizallah Izady⁵

6 ¹School of Agriculture and Environment, The University of Western Australia, 35 Stirling Hwy,
7 Crawley, Perth WA, 6009, Australia

8 ²School of Ecosystem and Forest Sciences, The University of Melbourne, Richmond, VIC, 3121,
9 Australia

10 ³School of Life Sciences University of Technology Sydney Broadway NSW 2007

11 ⁴OzFlux Central Node, TERN Ecosystem Processes, Melbourne, VIC 3159, Australia

12 ⁵Water Research Center, Sultan Qaboos University, Muscat, Oman

13

14 *Correspondence to:* Atbin Mahabbati (atbin.m@hotmail.com)

15

16 Abstract

17

18 The errors and uncertainties associated with gap-filling algorithms of water, carbon and energy fluxes
19 data, have always been one of the main challenges of the global network of microclimatological tower
20 sites that use eddy covariance (EC) technique. To address these concerns, and find more efficient gap-
21 filling algorithms, we reviewed eight algorithms to estimate missing values of environmental drivers,
22 and separately, nine algorithms for the three major fluxes in EC time series. We then examined the
23 algorithms' performance for different gap-filling scenarios utilising the data from five EC towers during
24 2013. This research's objectives were a) to evaluate the impact of the gap lengths on the performance of
25 each algorithm; b) to compare the performance of traditional and new gap-filling techniques for the
26 EC data, for fluxes and separately for their corresponding meteorological drivers. The algorithms'
27 performance was evaluated by generating nine gap windows with different lengths, ranging from a day
28 to 365 days. In each scenario, a gap period was chosen randomly, and the data were removed from the
29 dataset, accordingly. After running each scenario, a variety of statistical metrics were used to evaluate
30 the algorithms' performance. The algorithms showed different levels of sensitivity to the gap lengths; The
31 Prophet Forecast Model (FBP) revealed the most sensitivity, whilst the performance of artificial neural
32 networks (ANNs), for instance, did not vary as much by changing the gap length. The algorithms'
33 performance generally decreased with increasing the gap length, yet the differences were not significant
34 for the windows smaller than 30 days. No significant difference between the algorithms was recognised for
35 the meteorological and environmental drivers. However, the linear algorithms showed slight superiority
36 over those of machine learning (ML), except the random forest algorithm estimating the ground heat
37 flux (RMSEs of 28.91 and 33.92 for RF and CLR respectively). However, for the major fluxes, ML

38 algorithms and the MDS showed superiority over the other algorithms. Even though ANNs, random
39 forest (RF) and extreme gradient boost (XGB) showed comparable performance in gap-filling of the
40 major fluxes, RF provided more consistent results with slightly less bias, as against the other ML
41 algorithms. The results indicated that there is no single algorithm which outperforms in all situations,
42 but the RF is a potential alternative for the ANNs as regards flux gap-filling.

43

44 1. Introduction

45 To address the global challenges of climatological and ecological changes, environmental
46 scientists and policymakers are demanding data that are continuous in time and space. Besides, there
47 is a need for quantifying and reducing uncertainties in such data, including observations of carbon,
48 water and energy exchanges that are crucial components in national/international flux networks and
49 global earth observing systems. Satellites partially fill this gap as they provide excellent spatial
50 coverage but at a limited temporal resolution, and not measured at a point scale. As such, high-quality
51 long-term site observations of ecosystem process and fluxes are needed that are continuous in time
52 and space. The global eddy covariance (EC) flux tower networks (FLUXNET), consisted of its regional
53 counterparts (i.e. AmeriFlux, EUROFLUX, OzFlux, etc.), was established in the late 1990s to address
54 the global demand for such information (Aubinet et al., 1999; Baldocchi et al., 2001; Beringer et al.,
55 2016a; Hollinger et al., 1999; Menzer et al., 2013; Tenhunen et al., 1998). Despite EC data being
56 frequently used to validate process modelling analyses, field surveys and remote sensing assessments
57 (Hagen et al., 2006), there are some serious concerns regarding the challenges associated with the
58 technique, e.g. data gaps and uncertainties. Hence, filling data gaps and reducing uncertainties
59 through better gap-filling techniques are highly needed.

60 Even though the EC is a common technique to measure fluxes of carbon, water and energy,
61 there are some challenges in providing robust, high-quality continuous observations. One of the
62 challenges regarding the technique, and therefore, the flux networks, is addressing data gaps and the
63 uncertainties associated with the gap-filling process, mainly when the gap windows are long (longer
64 than 12 consecutive days, as described by (Moffat et al., 2007)). These gaps happen very often due to
65 a variety of reasons, such as values out of range, spike detection or manual exclusion of date and time
66 ranges, instrument or power failure, herbivores, fire, eagles nests, cows, lightning, researchers on
67 leave, etc. (Beringer et al., 2016b). Since EC flux towers are often located in harsh climates, their data
68 are more susceptible to adverse weather (i.e. rain conditions), and they sometimes prevent quick
69 access to sites for repair and maintenance. As a result, this issue can, in turn, produce gaps which
70 might be relatively long (Isaac et al., 2017), and thus, problematic as follows. Firstly, loss of data is
71 considered a threat to scientific studies depending on the missing data quantity, pattern, mechanism
72 and nature (Altman and Bland, 2007; Molenberghs et al., 2014; Tannenbaum, 2010). That is because
73 using an incomplete dataset might lead to biased, invalid and unreliable results (Allison, 2000; Kang,
74 2013; Little, 2002). Second, continuous gap-filled data are required to calculate the annual or monthly
75 budgets of carbon or water balance components (Hutley et al., 2005).

76 Other than the challenges caused by missing data, there are several sources of errors and
77 uncertainties in the EC technique. Firstly, random error is associated with the stochastic nature of
78 turbulence, associated sampling errors (incomplete sampling of large eddies, uncertainty in the
79 calculated covariance between the vertical wind velocity and the scalar of interest), instrument errors,
80 and footprint variability (Aubinet et al., 2012a). For instance, Dragoni et al. (2007) analysed an EC-
81 based data of Morgan-Monroe State Forest for eight years (1999-2006) and assessed that instrument
82 uncertainty was equal to 3 % of the total annual NEE. Another primary source of uncertainty in EC
83 measurements is systematic errors that are usually caused by methodological challenges and
84 instrument calibration problems (e.g. sonic anemometer errors, spikes, gas analyser errors, etc.).
85 Finally, one of the sources of uncertainties is data processing, especially data gap-filling (Isaac et al.,
86 2017; Moffat et al., 2007; Richardson et al., 2012; Richardson and Hollinger, 2007).

87

88 There are several uncertainties pertaining to gap-filling of missing values, including
89 measurement uncertainty (Richardson and Hollinger, 2007), lengths and timing the gaps (Falge et al.,
90 2001; Richardson and Hollinger, 2007) and the particular gap-filling algorithm that is used (Falge et
91 al., 2001; Moffat et al., 2007). However, there are two dominant issues of long data gaps and the choice
92 of a particular gap-filling algorithm (Aubinet et al., 2012a). Firstly, long gaps can significantly increase
93 the total amount of uncertainty as the ecosystem behaviour might change because of different
94 agricultural periods or phenological phases (e.g. growing season, harvest period, bushfire, etc.). And
95 thereby show different responses under similar meteorological conditions (Aubinet et al., 2012a; Isaac
96 et al., 2017; Richardson and Hollinger, 2007). Consequently, the period in which a long gap happens
97 is essential. For example, research undertaken by Richardson & Hollinger (2007) on data from a range
98 of FLUXNET sites revealed that a week data gap during spring green-up in a forest led to a higher
99 uncertainty over a three-week gap period during winter. Second, each gap-filling algorithm has its
100 strengths and weaknesses; for instance, Moffat et al. (2007) compared 15 different commonly-used
101 gap-filling algorithms. They found that there was not a significant difference between the
102 performances of the algorithms with “good” reliability based on analysis of variance of RMSE.
103 Besides, the overall gap-filling uncertainty was within $\pm 25 \text{ g C m}^{-2} \text{ yr}^{-1}$ for most of the proper
104 algorithms, whereas, the other algorithms generated higher uncertainties of up to $\pm 75 \text{ g C m}^{-2} \text{ yr}^{-1}$,
105 showing that the uncertainty provided by reliable methods can be considerably smaller. This result is
106 similar to the findings of Richardson & Hollinger (2007) who found as for the datasets used in the
107 study, uncertainties of up to $\pm 30 \text{ g C m}^{-2} \text{ yr}^{-1}$ for long gaps by appropriate algorithms. Considering that
108 the data provided by EC tower networks are of use for research, government and policymakers, robust
109 gap-filling is a need to quantify and reduce uncertainties in flux estimations.

110

111 To manage the missing data problem, several methods have been typically used to fill data
112 gaps in both fluxes and their meteorological drivers. Due to computational constraints of complex
113 algorithms, early works to impute EC data gaps used interpolation methods based mostly on linear
114 regression or temporal autocorrelation (Falge et al., 2001; Lee et al., 1999). These approaches were

115 replaced quickly by more sophisticated methods such as non-linear regressions (Barr et al., 2004; Falge
116 et al., 2001; Moffat et al., 2007; Richardson et al., 2006); lookup tables (Falge et al., 2001; Law et al.,
117 2002; Zhao and Huang, 2015); artificial neural networks (ANNs) (Aubinet et al., 1999; Beringer et al.,
118 2016a; Cleverly et al., 2013; Hagen et al., 2006; Isaac et al., 2017; Kunwor et al., 2017; Moffat et al., 2007;
119 Papale and Valentini, 2003; Pilegaard et al., 2001; Staebler, 1999); mean diurnal variation (Falge et al.,
120 2001; Moffat et al., 2007; Zhao and Huang, 2015), multiple imputations (Hui et al., 2004; Moffat et al.,
121 2007), etc. Each of these methods has its pros and cons as follows: a) Interpolation methods such as
122 the Mean Diurnal Variation (MDV), do not need any drivers, yet, their accuracy is lower than other
123 approaches (Aubinet et al., 2012a). Moreover, this method may provide biased results on extremely
124 clear or cloudy days (Falge et al., 2001). MDV is not recommended when a gap is longer than two
125 weeks, for it cannot consider the non-linear relations between the drivers and the flux, and thus leads
126 to a high level of uncertainty (Falge et al., 2001). And b) The Lookup table, especially its modified
127 version, Marginal Distribution Sampling (MDS), has provided performance close to ANNs, and are
128 more reliable and consistent than the other algorithms so far. Hence, MDS was chosen as one of the
129 standard gap-filling methods in EUROFLUX (Aubinet et al., 2012a). Nevertheless, one of the concerns
130 regarding this algorithm is that the independent variables, here meteorological drivers, might be auto-
131 correlated. c) ANNs have commonly been used to gap-fill EC fluxes since 2000 and because of their
132 robust and consistent results are considered as a standard gap-filling algorithm in several networks,
133 e.g. ICOS, FLUXNET, OzFlux, etc. (Aubinet et al., 2012a; Beringer et al., 2017; Isaac et al., 2017). Despite
134 their reliable performance, ANNs –and generally all other ML algorithms– face some challenges. Over-
135 fitting, for instance, is a big concern and can happen when the number of degrees of freedom is high,
136 while the training window is not long enough respectively, or the quality of the training dataset is
137 low. This challenge becomes acute when the gaps happen within a period when the ecosystem
138 behaviour is changing and thereby showing different response under similar meteorological
139 conditions. Furthermore, there is a desire to have the training windows short so that the algorithm
140 can track the ecosystem behaviour shift. Yet, this increases the risk of over-fitting depending on the
141 algorithm. In other words, the training window length should be neither too short to cause over-
142 fitting, and nor too long to lead algorithms to ignore ecological condition changes. Besides, long gaps
143 are considered as one of the primary uncertainty sources of CO₂ flux in the FLUXNET (Aubinet et al.,
144 2012a). As a result, studying the effects of the gap lengths, as well as the window length whereby an
145 algorithm is trained are both critical challenges associated with the environmental data gap-filling.

146

147 Apart from the limitations and disadvantages of the mentioned algorithms, gap-filling of fluxes (i.e.
148 NEE) experiences some other challenges that make it necessary to find or develop new gap-filling
149 algorithms. That is because the current methods are not flexible enough to perform well in special
150 occasions or extreme values (Kunwor et al., 2017), and there is almost no room to optimise them to
151 improve their outcome (Moffat et al., 2007). Moreover, even using the best available algorithm, such
152 as ANNs, the model (gap-filling) uncertainty still accounts for a sizable proportion of the total
153 uncertainties, especially when the gaps are relatively long. Since the 2000s when MDS and ANNs were
154 chosen as the most reliable gap-filling methods for EC flux observations, many new ML and

155 optimisation algorithms have been developed and used in varieties of scientific fields. Some of which
156 have shown superiority over ANNs, either individually or as a part of a hybrid or ensemble model,
157 e.g. (Gani et al., 2016). As a result, comparing the cutting-edge algorithms with the current standard
158 ones can show whether there is any room to improve the gap-filling process within the field.
159 According to the concerns mentioned above, this paper had two objectives. a) To find out the impact
160 of different window lengths on the performance of each algorithm. And b) to evaluate the
161 performance of traditional and new gap-filling techniques, separately for fluxes and their
162 meteorological drivers, particularly soil moisture, for this has always been a challenging variable to
163 gap-fill for a couple of reasons, such as of the biology and heterogeneity of soil parameters. To address
164 these objectives, we utilised nine different algorithms (Extreme Gradient Boost (XGB), Random Forest
165 Algorithm (RF), Artificial Neural Networks (ANNs), Marginal Distribution Sampling (MDS), Classic
166 Linear Regression (CLR), Support Vector Regression (SVR), Elastic net regularisation (ELN), Panel
167 Data (PD) and Prophet Forecast Model (FBP)) to fill the gaps of the major fluxes, and eight of them
168 (excluding MDS) to fill the gaps of the environmental drivers. We then assessed their relative
169 performance to evaluate potentially better ways to fill EC flux data. To test the approaches, we used
170 five flux towers from the OzFlux network. To evaluate the performance of these algorithms, nine
171 scenarios for gaps were planned – from a day to a whole year - and applied to the datasets, and
172 different common performance metrics (e.g. RMSE, MBE, etc.), as well as visual graphs were used.
173

174 2. Materials and methods

175

176 To address the first objective of this research, nine different gap lengths were superimposed to
177 the datasets, i.e. 1, 5, 10, 20, 30, 60, 90, 180 and 365 days. To address the second objective, we chose
178 nine different algorithms to fill the gaps, including a wide variety of different approaches, e.g. from a
179 simple algorithm like CLR to cutting-edge ML algorithms, such as XGB (MDS was not used for the
180 environmental drivers). The data used in this paper came from five EC towers of the OzFlux Network,
181 i.e. Alice Springs Mulga, Calperum, Gingin, Howard Springs and Tumbarumba from 2012 to 2013,
182 with a time resolution of 30 minutes, except for Tumbarumba (60 minutes). Additionally, data coming
183 from three additional sources outside of the network were also used as ancillary data to help the
184 algorithms fill the gaps of environmental drivers.

185 2.1. Data

186 The data used for this research came from OzFlux, which is the regional Australian and New
187 Zealand flux tower network that aims to provide a continental-scale national research facility to
188 monitor and assess Australia's terrestrial biosphere and climate (Beringer et al., 2016a). As described
189 in (Isaac et al., 2017), all OzFlux towers continuously measure and record 28 environmental features
190 at resolutions up to 10 Hz, and use a 30 min averaging period, with a few exceptions (data are available
191 from (<http://data.ozflux.org.au/portal>)). Besides, the network acquires additional data from the
192 Australian Bureau of Meteorology (BoM), the European Centre for Medium-Range Weather
193 Forecasting (ECMWF), and the Moderate Resolution Imaging Spectroradiometer (MODIS) on the
194 TERRA and AQUA satellites (Isaac et al., 2017). These additional data, also known as ancillary data,
195 provide alternative data for gap-filling flux tower datasets (Isaac et al., 2017). As explained in (Isaac
196 et al., 2017), OzFlux uses the BoM automated weather station (AWS) datasets to gap-fill the

197 meteorological data, the BoM weather forecasting model (ACCESS-R) for radiation and soil data from
 198 2011 onward, and MODIS MOD13Q1 for Normalised Difference Vegetation Index (NDVI) and
 199 Enhanced Vegetation Index (EVI). Moreover, the data provided by BIOS2, a physically-based model-
 200 data integration environment for tracking Australian carbon and water (Haverd et al., 2015), were also
 201 used as another ancillary source for varieties of environmental features. Current ACCESS-R and
 202 MODIS data are available from the BoM OPeNDAP (<http://www.opendap.org/>) server and TERN-
 203 AusCover data (<http://www.auscover.org.au/>), respectively.

204
 205 The datasets were used in this research came from five towers amongst the OzFlux Network
 206 between 2012 and 2013, each representative of a different climate and land cover of Australian
 207 ecological conditions; i.e. Alice Springs Mulga: Tropical and Subtropical Desert, Calperum: steppe,
 208 Gingin: Mediterranean, Howard Springs: Tropical Savanna, Tumbarumba: Oceanic (Table 1)
 209 (Beringer et al. 2016). The datasets included 15 meteorological drivers as well as three major fluxes
 210 recorded (Table 2) based upon EC technique at a 30-minute temporal resolution, except for
 211 Tumbarumba, which was hourly. Additionally, relevant ancillary datasets for the mentioned towers
 212 were used to follow the OzFlux Network gap-filling protocol. Each dataset was quality checked at
 213 three levels based on the OzFlux Network protocol described in (Isaac et al., 2017) and applied using
 214 PyFluxPro ver. 0.9.2. To address the underestimation of canopy respiration by EC measurements at
 215 night, we used the CPD method of (Barr et al., 2013) to reject nightly records when the friction velocity
 216 fell below the threshold value of each site. After dismissing the inappropriate measurements, overall
 217 coverage of 72-88 % and 21-48 % were achieved for diurnal and nocturnal records during 2013 (the
 218 year to which the artificial gaps were superimposed), respectively.

219
 220 *Table 1. The information of the five towers that their data were used, including their name, location, dominant species and*
 221 *climate.*

Site	Location	Species	Climate	Latitude, Longitude (degree)
Alice Springs Mulga [AU-ASM]	Pine Hill cattle station, near Alice Springs, Northern Territory	Semi-arid mulga (Acacia aneura) ecosystem	Tropical and Subtropical Desert Climate (Bwh)	-22.2828° N, 133.2493° E
Calperum [AU-Cpr]	Calperum Station, 25 km NW of Renmark, South Australia	Recovering Mallee woodland	Steppe Climate (Bsk)	-34.0027° N, 140.5877° E
Gingin [AU-Gin]	Swan Coastal Plain 70 km north of Perth, Western Australia	Coastal heath Banksia woodland	Mediterranean Climate (Csa)	-31.3764° N, 115.7139° E
Howard Springs [AU-How]	E of Darwin, NT	Tropical savanna (wet)	Tropical Savanna Climate (Aw)	-12.4943° N, 131.1523° E
Tumbarumba [AU- Tum]	Near Tumbarumba, NSW	Wet temperate sclerophyll eucalypt	Oceanic climate (Cfb)	-35.6566° N, 148.1517° E

222

223 *Table 2. List of variables and their units used in this research, including the three main fluxes and their environmental drivers.*

List of variables	Units
Drivers:	
Ah	Absolute Humidity (g m^{-3})
Fa	Available energy (W m^{-2})
Fg	Ground heat flux (W m^{-2})
Fld	Downwelling long-wave radiation (W m^{-2})
Flu	Upwelling long-wave radiation (W m^{-2})
Fn	Net radiation (W m^{-2})
Fsd	Downwelling short-wave radiation (W m^{-2})
Fsu	Upwelling short-wave radiation (W m^{-2})
ps	Surface pressure (kPa)
Sws	Soil water content (m m^{-1})
Ta	Air temperature (C)
Ts	Soil temperature (C)
Ws	Wind speed (m s^{-1})
Wd	Wind direction (deg)
Precip	Precipitation (mm)
q	Specific Humidity (kg kg^{-1})
Fluxes:	
Fc (also NEE)	CO ₂ flux ($\mu\text{mol m}^{-2} \text{s}^{-1}$)
Fh (also H)	Sensible heat flux (W m^{-2})
Fe (also LE)	Latent heat flux (W m^{-2})

224
 225 The datasets whereby each environmental variable was gap-filled are shown in Table 3. For each of
 226 these variables, the same variable of the ancillary source was used to fill the gaps. For instance, to gap-
 227 fill Ah, the Ah records of AWS, ACCESS-R and BIOS2 were used. To gap-fill the missing values of
 228 fluxes, i.e. Fc (NEE), Fh (H) and Fe (LE), eight drivers were used as follows: Ta, Ws, Sws, Fg, VPD, Fn,
 229 q and Ts based on a combination of RF feature selection and testing out a series of feature
 230 combinations. Different libraries of Python Programming Language (ver. 3.6.4) were utilised for
 231 training and testing the algorithms, i.e. xgboost for XGB, fbprophet for FBP, statsmodels for PD and
 232 sklearn for the rest of algorithms. Each algorithm was tuned up individually using grid search, and
 233 the number of nodes, layers, irritations, etc. were chosen therefor.

234
 235
 236 *Table 3. The ancillary sources whereby each environmental driver was gap-filled.*

List of variables (y)	Ancillary Source
Drivers:	
Ah	AWS, ACCESS-R, BIOS2
Fa	ACCESS-R, BIOS2
Fg	ACCESS-R, BIOS2
Fld	ACCESS-R, BIOS2
Flu	ACCESS-R, BIOS2
Fn	ACCESS-R, BIOS2
Fsd	ACCESS-R, BIOS2
Fsu	ACCESS-R, BIOS2
ps	AWS, ACCESS-R

Sws	ACCESS-R, BIOS2
Ta	AWS, ACCESS-R, BIOS2
Ts	ACCESS-R, BIOS2
Ws	AWS, ACCESS-R
Wd	AWS, ACCESS-R
Precip	AWS, ACCESS-R, BIOS2

237
238

239 *2.2. Gap-filling algorithms*

240
241
242
243
244
245
246

Eight imputation algorithms for estimating 15 environmental drivers and 9 algorithms for the 3 major fluxes were picked out to make the comparison. These algorithms were used in a way that a variety of approaches were tested, from the standard methods like ANNs and MDS, to the newer algorithms which rarely or never been used in the field, such as Extreme Gradient Boosting and panel data.

247 **Marginal Distribution Sampling (MDS)**

248 As introduced by Reichstein (Reichstein et al., 2005), the MDS is an enhanced Look-up Tables
249 method, which considers both the covariation of fluxes with meteorological variables and the
250 temporal auto-correlation of the fluxes (Aubinet et al., 2012b). Alongside the ANNs, the MDS is
251 considered as one of the standard gap-filling methods for flux data amongst the FLUXNET, and is
252 selected in this study to help the community to have a clear idea of the performance of other
253 algorithms. Unlike the other algorithms used in this research, we used Fsd, Ta and VPD as the input
254 features for the MDS. The PyFluxPro ver. 0.9.2 was used to apply the algorithm (modified code used
255 for the gaps longer than 10 days).
256

257 **Artificial Neural Networks (ANN)**

258 Rooted in the 1950s, artificial neural networks are ML methods inspired by biological neural
259 networks and are classified as supervised learning methods (Dreyfus, 1990; Farley and Clark, 1954).
260 ANN work based on several connected units called nodes, which are used to mimic the functionality
261 of a neuron in an animal brain by sending and receiving signals to other nodes. The ANN technique
262 used in this paper was Multi-layer Perceptron regressor, which optimises the squared-loss using
263 stochastic gradient descent. Sklearn.neural_network.MLPRegressor was used to apply this method
264 in Python, and its hyperparameters were 800 and 500 for “hidden_layer_sizes” and “max_iter”,
265 respectively based on grid search. ANN are one of the current standard approaches for gap-filling in
266 FLUXNET and in this research were picked out as a performance reference for other algorithms.

267
268 **Classical Linear Regression (CLR)**

269 A classical linear regression is an equation developed to estimate the value of the dependent
270 variable (y) based on independent values (x_i). In contrast, each x_i has its specific coefficient and an
271 overall intercept value. In this method, these coefficients are determined by minimising the squared
272 residuals (errors) of estimated vs observed values, called least squares. A CLR algorithm can be
273 formulated as follows (Freedman, 2009):

$$y = \alpha + \beta_1 X_1 + \beta_2 X_2 + \beta_3 X_3 + \dots + \beta_i X_i + \varepsilon \quad (1)$$

274 where y is the dependent variable, α is the interception, X_s are independent variables, and β_i is
275 coefficient of X_i , and ε is the error term. We chose this algorithm as a baseline to find out how better
276 more complicated algorithms can estimate dependent variables comparatively.

277 **Random Forests (RF)**

278 Random forest, a supervised ML algorithm, used for both classification and regression,
279 consists of multiple trees constructed systematically by pseudorandomly selecting subsets of
280 components of the feature vector, that is, trees constructed in randomly chosen subspaces (Ho, 1998).
281 RF algorithm has been developed to control the overcome over-fitting problem, a commonplace
282 limitation of its preceding decision tree-based methods (Ho, 1995, 1998).
283 Sklearn.ensemble.RandomForestRegressor was used to apply this method in Python, and the
284 hyperparameters used were 5 and 1000 for “max_depth” and “n_estimators”, respectively based on
285 grid search.

286 287 **Support Vector Regression (SVR)**

288 As a non-linear method, support vector regression was developed based on Vanpik’s concept
289 of support vectors theory (Drucker et al., 1997). An SVR algorithm is trained by trying to solve the
290 following problem:

291

$$292 \text{ minimise } \frac{1}{2} \|w\|^2$$

293 subject to $\begin{cases} y_i - \langle w, x_i \rangle - b \leq \varepsilon, \\ \langle w, x_i \rangle + b - y_i \leq \varepsilon, \end{cases}$

294 where x_i and y_i are training sample and target value in a row. The inner product plus intercept
295 $\langle w, x_i \rangle + b$ is the prediction for that sample, and ε is a free parameter that serves as a threshold.
296 sklearn.svm.SVR was used to apply this method in Python, and the hyperparameters that used were
297 1 and 0.001 for “C” and “gamma”, respectively based on grid search.

298 **Elastic net regularisation (ELN)**

299 The elastic net is a linear regularised regression method that exerts small amounts of bias by
300 adding two penalty components to the regressed line to decline the coefficients of independent
301 variables and thus, provides better long-term predictions. Given that these two penalty components

302 come from ridge regression and LASSO, the elastic net is considered as a hybrid model consists of
 303 ridge and LASSO regressions, overcoming the limitations of both. The estimates from the ELN method
 304 can be formulated as below (Zou and Hastie, 2005):

$$\hat{\beta}(\text{elastic net}) = \frac{(|\hat{\beta}(OLS)| - \lambda_1/2)}{1 + \lambda_2} \text{sgn}\{\hat{\beta}(OLS)\} \quad (2)$$

305
 306 where $\hat{\beta}$ is the coefficient of each ELN independent variable, λ_1 and λ_2 are penalty coefficients of
 307 LASSO and ridge regression respectively, $\hat{\beta}(OLS)$ is the coefficient of an independent variable
 308 calculated based on ordinary least squares, and sgn stands for the sign function:

$$\text{sgn}(x) = \begin{cases} 1 & x > 0 \\ 0 & x = 0 \\ -1 & x < 0 \end{cases} \quad (3)$$

309
 310 The ELN regression is good at addressing situations when the training datasets have small samples
 311 or when there are correlations between parameters. `sklearn.linear_model.ElasticNet` was used to
 312 apply this method in Python, and the hyperparameters used were as follows: {'alpha': 0.01,
 313 'fit_intercept': True, 'max_iter': 5000, 'normalize': False} based on grid search.

314
 315 **Panel data (PD)**

316 Panel data is a multidimensional statistical method, mainly used in econometrics to analyse
 317 datasets, which involve time series of observations amongst individual cross-sections (Baltagi, 1995)
 318 usually based on ordinary least squares (OLS) or generalised least squares (GLS). A two-way panel
 319 data model consists of two extra components above a CLR as follows (Baltagi, 1995; Hsiao et al., 2002;
 320 Wooldridge, 2008):

$$y_{it} = \alpha + \beta X_{it} + u_{it} \quad i = 1, 2, \dots, N; \quad t = 1, 2, \dots, T \quad (4)$$

$$y_{it} = \alpha + \beta X_{it} + \mu_i + \lambda_t \quad (5)$$

321 where i and t denote the cross-section and time series dimension in a row, y is a dependent-variable
 322 vector, X is an independent variable matrix, α is a scalar, β is the coefficient of the independent-
 323 variable matrix, μ_i is the unobservable individual-specific effect, and λ_t is the unobservable time-
 324 specific effect. Panel data abilities to provide a holistic analysis of different individuals, as well as
 325 determining the specific impact of every single time caused its superiority over CLR. Since PD requires
 326 cross-sections to be applied, we used a cross-section tower for each of the main five tower as follows:
 327 Ti Tree East for Alice Springs Mulga, Whroo for Calperum, Great Western Woodlands for Gingin,
 328 Daly River for Howard Springs, and Cumberland Plain for Tumbarumba. The cross-section towers
 329 were chosen based on their distances (the closest ones with common years of data).

330 **Extreme Gradient Boost (XGB)**

331 Extreme gradient boost is a reinforced method of Gradient Boost introduced in 1999 that
332 works based on parallel boosted decision trees and similar to RF can be used for a variety of data
333 processing purposes including classification and regression (Friedman, 2002; Jerome H. Friedman,
334 2001; Ye et al., 2009). XGB method is resistive to over-fitting and provides a robust, portable and
335 scalable algorithm for large-scale boosting decision-trees-based techniques.
336 `sklearn.ensemble.GradientBoostingRegressor` was used to apply this method in Python, and its
337 hyperparameters were chosen based on grid search as follows: {'learning_rate': 0.001, 'max_depth': 8,
338 'reg_alpha': 0.1, 'subsample': 0.5}.

339

340 **The Prophet Forecasting Model (FBP)**

341 The Prophet Forecasting Model, also known as “prophet”, is a time series forecasting model
342 developed by Facebook to manage the common features of business time series and designed to have
343 intuitive parameters that can be adjusted without knowing the details of underlying model (Taylor
344 and Letham, 2017). A decomposable time series model was used (Harvey and Peters, 1990) to develop
345 this model, with three main components: trend, seasonality, and holidays as the equation below
346 (Taylor and Letham, 2018):

$$y(t) = g(t) + s(t) + h(t) \quad (6)$$

347

348 where $g(t)$ is the trend function, which models non-periodic changes, $s(t)$ is a function to represent
349 periodic changes, e.g. seasonality, and $h(t)$ assesses the effects of potential anomalies which occur over
350 one or more days, e.g. holidays.

351

352 *2.3. The gap scenarios*

353 In order to find out the effect of gap size on the performance of our gap-filling algorithms, the
354 data of nine different gap windows (i.e. 1, 5, 10, 20, 30, 60, 90, 180 and 365 consecutive days) were
355 removed randomly from the datasets during 2013. Afterwards, the data from 2012 to 2013 were used
356 to train the algorithms. Finally, the trained algorithms were used to fill the artificial gaps
357 superimposed to the datasets. The entire process permuted five times in each scenario to ensure the
358 performance was not sensitive to the gap period. As such, 15 variables, 9 window lengths, 8 gap-filling
359 methods (MDS excluded), and 5 permutations across 5 towers resulted in 27000 computations for the
360 meteorological features. Similarly, 3 fluxes, 9 window lengths, 9 gap-filling methods, and 5
361 permutations across 5 towers resulted in 6075 computations for the major fluxes, overall.

362 *2.4. Statistical performance measures*

363 Different statistical metrics were used to evaluate the performance of algorithms and enable
 364 comparison between measured values from the flux towers with each gap-filling algorithm prediction.
 365 These metrics included the coefficient of determination (R-squared) to measure the square of the
 366 coefficient of multiple correlations (Devore, 1991), the variance of measured and modelled values (S^2)
 367 to indicate how well algorithms could follow the variations of the recorded data, the root mean square
 368 error (RMSE), the mean bias error (MBE) to capture distribution and bias of residuals, variance ratio
 369 (VR) to compare the variance of estimated values with those of measured, and the Index of Agreement
 370 to compare the sum of the squared error to the potential error (Bennett et al., 2013). Abbreviations and
 371 formulas of these metrics are illustrated as follows (Bennett et al., 2013):

$$R^2 = \frac{[\sum(p_i - \bar{p})(o_i - \bar{o})]^2}{\sum(p_i - \bar{p})^2 \sum(o_i - \bar{o})^2} \quad (7)$$

$$S^2 = \frac{\sum(x_i - \bar{x})^2}{N - 1} \quad (8)$$

$$RMSE = \sqrt{\frac{\sum(p_i - o_i)^2}{N - 1}} \quad (9)$$

$$MBE = \frac{\sum o_i - p_i}{N - 1} \quad (10)$$

$$VR = \frac{\sigma_p^2}{\sigma_o^2} \quad (11)$$

$$IoAd = 1 - \frac{\sum_{i=1}^n (o_i - p_i)^2}{\sum_{i=1}^n (|p_i - \bar{o}| + |o_i - \bar{o}|)^2} \quad (12)$$

378 where o_i and p_i are individual measured and predicted values respectively, \bar{o} and \bar{p} are the means of
 379 o and p , and σ^2 is the variance. S^2 is calculated separately for the observed and predicted values with
 380 the respective values defined as x that represents every observed or predicted value. All of these
 381 metrics were calculated for each of the gap scenarios, and then the results of different windows were
 382 concatenated. Afterwards, the yearly metrics were calculated to avoid Simpson's paradox or any
 383 relevant averaging issue as described by (Kock and Gaskins, 2016). Moreover, the average of daily
 384 and seasonal differences between the estimated and measured values, as well as the associated
 385 variance were calculated and plotted.
 386

387 3. Results

388

389 3.1. Fluxes

390 3.1.1 Fc

391 Even though factors such as Fg and Fn are fluxes, we dealt with them as environmental drivers
392 since they drive the three major fluxes. The metrics used to evaluate the performance of the algorithms
393 (RMSE, R², MBE, IoAd and VR) (Table 4) illustrated that overall, the performance of these algorithms,
394 particularly the ML ones, was similar, closely followed by the MDS. The XGB provided the lowest
395 values of RMSE and one of the highest R², while the FBP and ELN had the lowest and highest values
396 of RMSE and R², respectively. The algorithms, however, showed different levels of sensitivity to the
397 gap lengths, e.g. the CLR and PD showed smaller sensitivity, while the FBP showed the most
398 sensitivity (Figure 1).

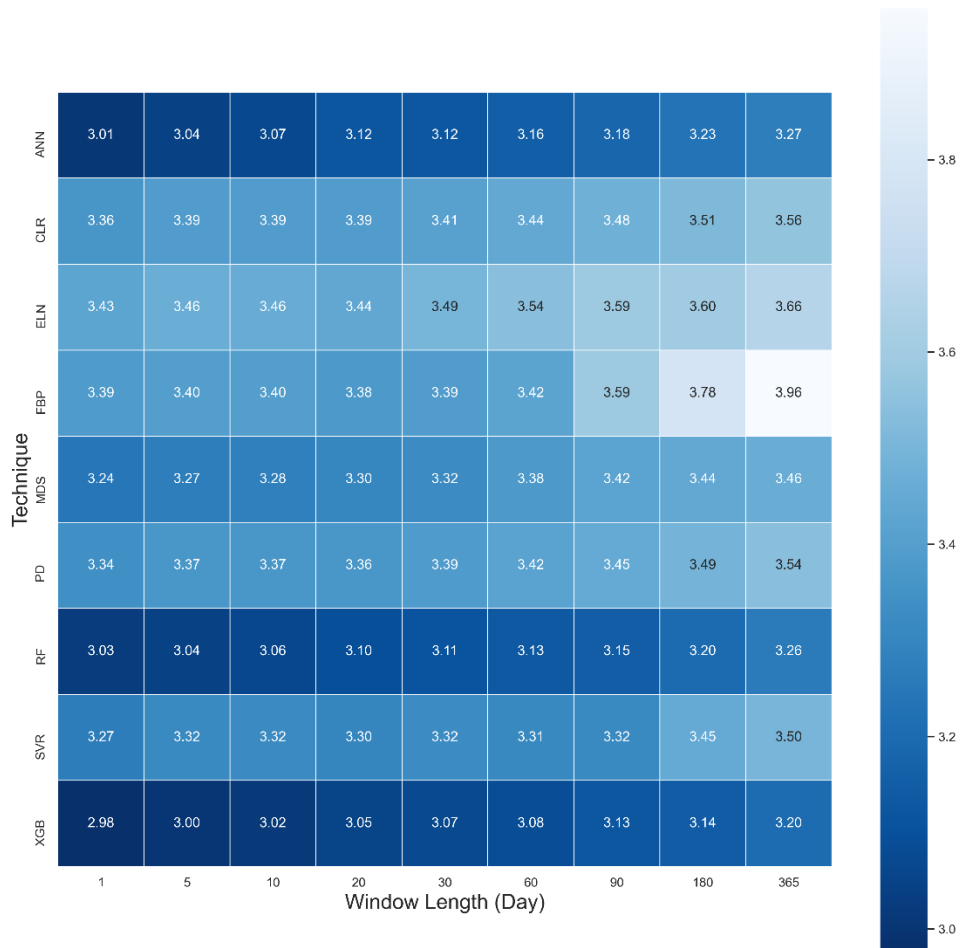
399 *Table 4. The average amounts of performance metrics for each gap-filling algorithm regarding Fc, which includes all window*
400 *lengths and sites, ranked by RMSE using the Tukey's HSD test at the level of 5 per cent.*

Algorithm	Mean RMSE	Mean R ²	Mean MBE	Mean IoAd	Mean VR
XGB	3.07 ^a	0.59	-0.43	0.90	0.66
RF	3.12 ^a	0.58	-0.37	0.91	0.71
ANNs	3.13 ^a	0.56	-0.33	0.90	0.69
SVR	3.34 ^b	0.47	-0.32	0.86	0.75
MDS	3.35 ^b	0.51	-0.41	0.85	0.70
PD	3.41 ^{b,c}	0.48	-0.35	0.81	0.54
CLR	3.44 ^{b,c}	0.49	-0.36	0.81	0.55
ELN	4.52 ^c	0.43	-0.37	0.73	0.39
FBP	4.15 ^d	0.47	-0.06	0.77	0.68

401

402 These outcomes were expected for the XGB as it uses a more regularised model formalisation to
403 control over-fitting (Chen and Guestrin, 2016) which, on paper, leads to better performance as against
404 its ML rivals. The relatively poor performance of FBP was also foreseen for unlike other algorithms,
405 FBP did not use any feature to estimate flux values, other than the previous time series of flux values.
406 However, the weaker performance of the ELN compared to CLR was unforeseen due to by adding
407 two penalty components to the regressed line, and the ELN is supposed to improve the long term
408 prediction compared to the traditional linear regression methods. Tukey's HSD (honestly significant
409 difference) test at the level of five per cent was applied to the results to find out whether the difference
410 amongst the algorithms was significant (Table 4). Where the null hypothesis was there is no significant
411 difference between the mean values of the RMSE. According to the results, there were significant
412 differences between certain algorithms, and the XGB, RF and ANNs were different from the rest,
413 showing that these three performed considerably better. Tukey's HSD test, however, did not reject the
414 second error probability between RF, XGB and ANNs meaning that the three algorithms were not
415 significantly different from each other. This result agrees with the results of (Falge et al., 2001) and
416 (Moffat et al., 2007) in the sense that ANNs are one of the best available gap-filling algorithms, and
417 there is no significant difference amongst the appropriate algorithms. However, the test showed that
418 the performance of the MDS had a significant difference from the ANNs. Finally, it is worth

419 mentioning that Tukey’s HSD is well known as a conservative test. That being said, despite no
 420 meaningful difference based on Tukey’s HSD, XGB and RF might have performed better than ANNs,
 421 as the superiority of RF in gap-filling of methane flux over the ANNs, SVR, and MDS has recently
 422 been claimed by (Kim et al., 2020).



423
 424 *Figure 1. A heat map of mean RMSE values of Fc across all sites based on 9 algorithms and 9 window lengths in 2013.*
 425

426 To address the first objective of this paper, finding out the sensitivity of the gap-filing
 427 algorithms to the gap window length, we used the averaged RMSE, R² and MBE for each gap size,
 428 using the output of all algorithms for all sites (Table 5). The outcome illustrates that the longer the

429 window length got, the bigger the amounts of RMSE became. Yet, no such pattern was recognisable
 430 for the R^2 and MBE. As a result, generally, any consecutive gaps longer than 30 days seem to decline
 431 the performance of the algorithms noticeably. The phenomenon can be justified by the idea that longer
 432 windows do not let the algorithms to accommodate seasonal changes and therefore, different
 433 physiological behaviour of the canopy.

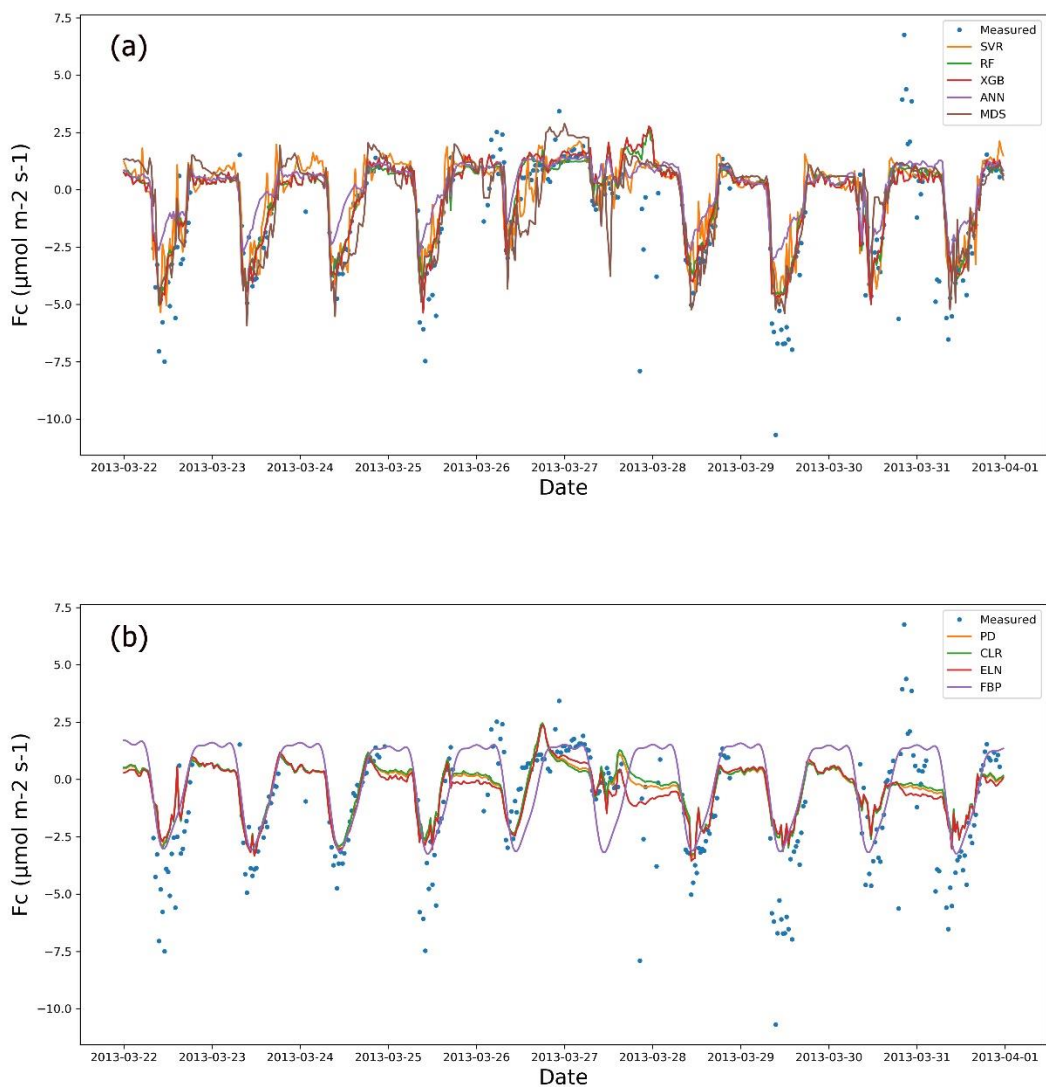
434 *Table 5. The average amounts of RMSE, R^2 , and MBE for Fc gap-filling based on the window length including the outcome of all*
 435 *sites; the differences of RMSE values were tested using the Tukey's HSD test at the level of 5 per cent.*

Window length	Mean RMSE	Mean R^2	Mean MBE
1-day	3.23 ^a	0.53	-0.27
5-days	3.25 ^a	0.52	-0.31
10-days	3.26 ^a	0.51	-0.29
20-days	3.27 ^a	0.51	-0.31
30-days	3.29 ^a	0.51	-0.31
60-days	3.32 ^a	0.49	-0.35
90-days	3.37 ^a	0.51	-0.38
180-days	3.43 ^a	0.50	-0.41
365-days	3.49 ^a	0.49	-0.37

436
 437 According to the MBE values (Table 4), mainly, all algorithms had negative amounts of MBE, showing
 438 overestimation of the Fc values. This bias varied from tower to tower and depended on the window
 439 lengths. For instance, absolute amounts of the MBE were bigger in Gingin and Tumberumba, while
 440 considerably smaller (closer to zero) at AliceSprings Mulga and Calperum (Supplementary). The
 441 lower leaf area index of the two later sites, and thus their smaller amounts of photosynthesis is likely
 442 to be the reason that justifies the outcome. FBP, nonetheless, provided substantially lower mean bias
 443 (-0.06) compared to the other algorithms, which varied between -0.32 and -0.43.

444 Observations from the EC technique often include extremely low or high values, especially at
 445 night, when some of the theoretical assumptions might be violated. The nature of the EC technique
 446 associated with its practical challenges, often makes it difficult to distinguish between the good data
 447 and the noise (Aubinet et al., 2012a; Burba and Anderson, 2010). This problem seems to affect the
 448 outcomes of the gap-filling algorithms in this research, as none of them performed ideally in capturing
 449 the observed variance (σ^2). Even though RMSE, R^2 and IoAd showed the superiority of the XGB, RF and
 450 ANNs, the variance ratio between the estimated and measured values revealed different information
 451 (Table 4), which is slightly recognisable in Figure 2. The variance ratios (VR) showed that SVR captured
 452 the extreme values of Fc better than the other algorithms, 0.75 on average. The other ML algorithms –

453 plus the MDS- though, performed closely with regard to capturing the extremes that matches both the
454 expectations, and the performance metrics Table 4.



455
456 *Figure 2. Measured vs estimated values of Fc for Calperum based on a 10-day gap window (March 22 - March 31, 2013).*

457 The linear algorithms, CLR, PD, and ELN, performed worse with respect to the VR compared to the
458 ML algorithms. The estimated versus measured values of Fc for Calperum () confirms the information
459 achieved by the VR. Based on the figure, the ELN, as expected, performed the worst in capturing the
460 fluctuations of Fc (VR = 0.39), while the performance of the other algorithms –apart from the top five-
461 was not considerably better, with the exception of FBP. It is noteworthy that CLR, PD, and ELN
462 frequently predicted nocturnal photosynthesis. Overall, the results showed a significant difference
463 between the top five algorithms (XGB, RF, ANNs, SVR, and MDS) and the others, particularly in
464 capturing the fluctuations and the min-max values of Fc. However, a comprehensive comparison
465 shows a slight superiority of the XGB and RF.

466
467
468
469
470
471
472
473
474
475
476
477
478
479
480
481
482
483
484
485

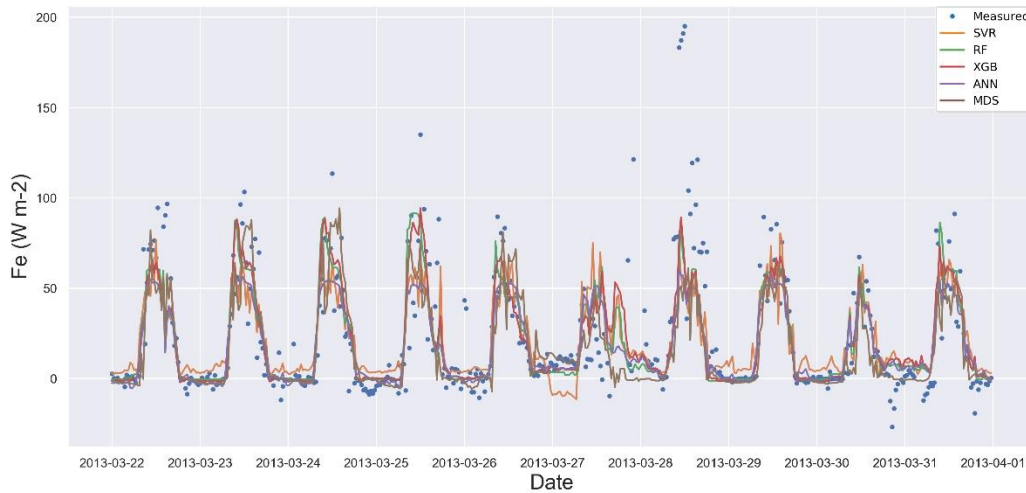
3.1.2 Fe

The performance of algorithms for Fe was similar to that for Fc regarding RMSE, MBE and R², as shown in Table 6. This similarity was not surprising since these processes are partially coupled via stomatal conductance (Scanlon and Kustas, 2010; Scanlon and Sahu, 2008). Again, the top three ML algorithms performed better, with a significant superiority of the XGB and RF, as shown by the Tukey’s HSD (Table 6), followed by the ANNs and MDS. Besides, the null hypothesis was not rejected while comparing FBP and SVR, whereas the better performance of the other algorithms was confirmed. As a result, the FBP and SVR provided the most unsatisfactory results in estimating Fe, according to the average values of the RMSE. No significant improvement in RMSE occurred when the gap lengths became shorter than 60 days, meaning that the performance of the algorithms did not vary considerably from a 30-day to a one-day window, especially for the top algorithms (XGB, RF, and ANNs). The results of CLR and PD were very similar to those for Fc, showed lower RMSE and higher R² values as against ELN, but the ELN led to slight lower MBE. The MBE values also showed moderately high values for the SVR, meaning that there was an absolute bias in its outcome, which might be related to overfitting. The source of the bias shown by the SVR algorithm (Figure 3), was because it could not capture the minimum values appropriately, resulting in a considerable overestimation. A common issue in estimating Fe values, which had affected all algorithms other than the FBP, was not assessing the negative values. In contrast to Fc results, the ANNs did not perform as solid as the XGB and RF, which could be due to not being able to capture the maximum values as satisfying as its rivals were.

486 *Table 6. The average of metrics for Fe gap-filling based on the algorithms, ranked by RMSE using the Tukey’s HSD test at the*
487 *level of 5 per cent.*

Algorithm (Fe)	Mean RMSE	Mean R ²	Mean MBE
XGB	34.95 ^a	0.74	-3.48
RF	35.63 ^a	0.74	-3.33
ANNs	37.77 ^{a,b}	0.67	-3.94
MDS	41.74 ^{b,c}	0.64	-3.27
PD	43.28 ^{b,c}	0.64	-6.35
CLR	43.51 ^c	0.64	-6.66
Eln	44.34 ^c	0.59	-5.13
SVR	46.63 ^{c,d}	0.59	-20.45
FBP	50.53 ^d	0.52	3.01

488
489



490
491 *Figure 3. Measured vs estimated values of Fe for Calperum based on a 10-day gap window (March 22 - March 31 2013).*

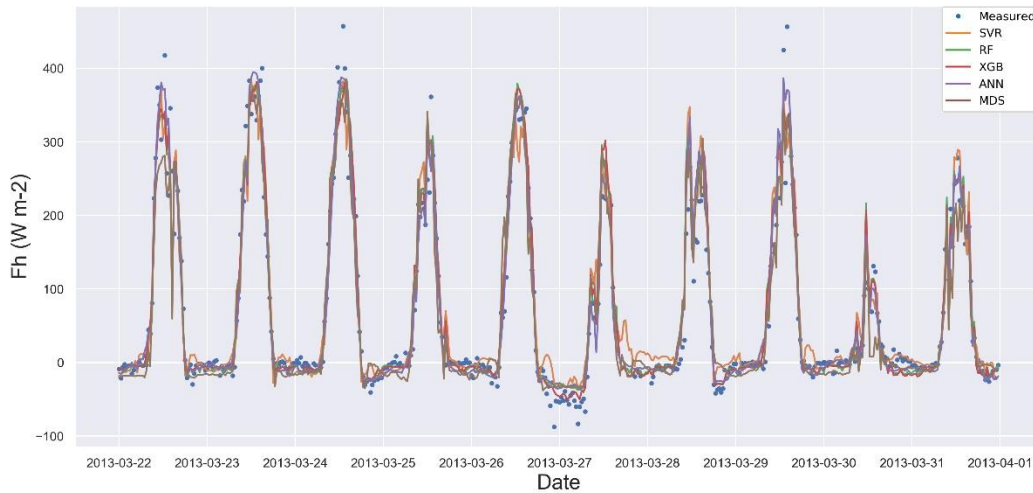
492

493 3.1.3 Fh

494 As with the other flux results, the metrics (RMSE, R² and MBE) showed slight superiority of
 495 XGB and RF, as well as the inferiority of the SVR and FBP over the other algorithms (Table 7).
 496 Likewise, the SVR provided relatively large negative values of MBE, showing considerable
 497 overestimation. The Tukey’s HSD test of the average RMSE values confirmed that the performance of
 498 the FBP was significantly different from the rest at the level of 5 per cent, making FBP the weakest
 499 performer for Fh. On the other hand, although there was no significant difference amongst the XGB,
 500 RF and ANNs, the first two were considerably superior over the other algorithms as regards the
 501 Tukey’s HSD test. Like Fe, estimated values of Fh using SVR had a negative bias (Figure 4) because it
 502 was not able to provide appropriate estimations of Fh minimum values. In contrast, the ANNs
 503 performed the best in capturing the minimum values, while the other top algorithms performed
 504 almost equally well. Despite the close performance in capturing the minimum values, ANNs and MDS
 505 did not carry out as solid as XGB and RF concerning the overall values, resulted in higher RMSE.
 506 Finally, similar to the other fluxes, the PD performed slightly better than the CLR and ELN.

507 *Table 7. The average metrics for Fh gap-filling based on the algorithms, ranked by RMSE using the Tukey’s HSD test at the level*
 508 *of 5 per cent.*

Algorithm (Fh)	Mean RMSE	Mean R ²	Mean MBE
XGB	37.23 ^a	0.92	-0.21
RF	37.55 ^a	0.91	-0.09
ANNs	40.13 ^{ab}	0.90	-0.08
MDS	43.30 ^{bc}	0.88	-9.51
SVR	43.80 ^{bc}	0.88	0.35
PD	44.96 ^c	0.88	1.36
CLR	45.03 ^c	0.88	1.64
ElN	45.19 ^c	0.87	2.16
FBP	72.91 ^d	0.73	1.07



509

510 *Figure 4. Measured vs estimated values of Fh for Calperum based on a 10-day gap window (March 22 - March 31 2013).*

511

512 *3.2. Meteorological and Environmental Drivers*

513 Since meteorological and environmental drivers are needed to fill the gaps of the three
 514 substantial fluxes, F_c , F_e and F_h , the eight algorithms (excluding the MDS) were used to fill the gaps
 515 of these drivers. The metrics of R^2 , RMSE, and MBE were calculated for all five towers and nine
 516 window lengths (16 meteorological and environmental drivers and three fluxes). Overall, for most
 517 meteorological drivers, the linear algorithms, especially the CLR and PD, performed slightly better
 518 than the ML algorithms such as the XGB, RF, ANNs and SVR, except for A_h , F_g and F_n . This
 519 unexpected superiority can be explained based on the two following reasons. Firstly, unlike the fluxes,
 520 the input and output features were the same here, e.g. T_a for T_a , which led to strong correlations (e.g.
 521 up to 0.99 for atmospheric pressure - ps) as well as strong linear relationships between the
 522 independent and dependent features. These strong correlations helped the linear algorithms to
 523 perform well, while nullified the ability of the ML algorithms to capture non-linear behaviour of
 524 complicated problems. Second, the slight inferiority of ML algorithms could be due to data noise
 525 where simple linear algorithms such as the CLR are usually less sensitive to the noise relatively.
 526 Therefore, over-fitting is not an issue for them when the number of observations is big enough (i.e. at
 527 least 10 to 20 observations per parameter (Harrell, 2014)). The exceptions were A_h , F_n and F_g , for
 528 which values were estimated more accurately by the XGB, ANNs and RF, especially the latest one (the
 529 RMSE of 28.91 versus 33.92 provided by the RF and CLR for F_g , respectively). Tukey's HSD test for
 530 the mean RMSE values of F_g confirmed that The XGB, ANNs and RF provided better results at the
 531 level of 5 per cent, while, like all other fluxes and drivers, the FBP confirmed to be the worst algorithm
 532 (Table 8). Yet, according to the same test for the other drivers, there was not any significant difference
 533 between the algorithms, other than the FBP, which provided the most significant mean values of the
 534 RMSE (results not shown). Importantly, though, none of the algorithms offered adequate estimations
 535 for soil moisture (S_{ws}), particularly in drier regions. This weak performance happened because S_{ws}

536 changes dramatically during rainfall in a pulsed manner often from zero to saturation in short space
 537 of time, whereas, the algorithms had been trained based on the datasets mostly reflecting non-rainy
 538 periods. These datasets, consequently, could not fit the algorithms in a way that they could estimate
 539 Sws accurately when precipitation occurs and the soil moisture increases dramatically. For instance,
 540 in a wet region like Tumbarumba, where the soil faces rainy days frequently, the time series are much
 541 less spikey. Thus, the overall performance was better in these regions compared with the drier ones,
 542 e.g. R^2 of 0.45 and 0.26 on average for Tumbarumba and Calperum, respectively. Besides, the dataset
 543 used to gap-fill the soil moisture was a model derivation from gridded data or regional reanalysis and
 544 therefore, can be not close to reality. Another challenge of estimating soil moisture comes from the
 545 low spatial coherence of soil moisture is that it can be extremely different just a couple of hundred
 546 metres away, due to storms, topography, soil structure heterogeneity, etc. (Reichle et al., 2004; Sahoo
 547 et al., 2008).

548

549 *Table 8. The average amounts of RMSE for Fg gap-filling based on the algorithms, using the Tukey's HSD test at the level of 5*
 550 *per cent.*

Algorithm (Fg)	Mean RMSE
RF ^a	28.91
XGB ^{a, b}	29.19
ANNs ^{b, c}	29.58
SVR ^c	31.46
CLR ^d	33.92
PD ^d	33.93
ELN ^d	34.09
FBP ^e	39.10

551

552 4. Discussion

553

554 *Table 9. The name and the abbreviation of the gap-filling algorithms.*

Algorithm abbreviation	Full name
XGB	Extreme Gradient Boost
RF	Random Forest Algorithm
ANNs	Artificial Neural Networks
MDS	Marginal Distribution Sampling
SVR	Support Vector Regressi
CLR	Classical Linear Regression
PD	Panel data
ELN	Elastic net regularisation
FBP	The Prophet Forecasting Model (Facebook Prophet)

555

556 All algorithms (Table 9) performed similarly in estimating the meteorological and
 557 environmental drivers (turbulent fluxes included) across all stations, except the FBP, which performed
 558 poorly for it did not use any ancillary data. The best results were achieved for the 30-day gaps and
 559 shorter, while the worst results obtained for the most extended windows, 180 and 365 days. Although

560 most of the algorithms performed almost equally well in estimating meteorological and
561 environmental drivers, the linear algorithms, the CLR, ELN and PD, performed slightly better (not
562 significant using a Tukey's HSD test, though). The only clear exception was Fg, for which the RF
563 provided more accurate and robust estimations. The ML algorithms and MDS, on the other hand,
564 showed their superiority over the linear algorithms while estimating the main fluxes, Fc, Fe and Fh.
565 For Fc, the XGB, RF and ANNs performed significantly better than the FBP and all linear algorithms,
566 i.e. the CLR, PD and ELN, yet, followed closely by the SVR and MDS. The superiority of the ML
567 algorithms, as well as their close performance, agreed with the results of previous researches, e.g.
568 (Falge et al., 2001; Moffat et al., 2007), that showed the superiority of non-linear algorithms and no
569 significant difference amongst the top algorithms in estimating Fc. Besides, the slight superiorities of
570 XGB and RF over ANNs, mainly unnoticeable by a conservative test like Tukey's HSD, confirms RF
571 performs better regarding the EC flux gap-filling (Kim et al., 2020).

572 The XGB was the most novel ML algorithm used in this research and based on the most
573 performance metrics provided comparatively robust results in estimating the fluxes. In estimating the
574 meteorological drivers though, the XGB did not show any superiority over the other algorithms,
575 especially the linear ones. Moreover, the XGB needed four to six times longer time to be trained and
576 tuned, making it a less feasible algorithm when time or the processing power are important factors
577 or several years of data are needed to be gap-filled. Hence, we do not recommend the XGB as an
578 alternative to the current alternative algorithms. Nevertheless, because of its local superiorities, this
579 algorithm might be suitable to use in an ensemble model alongside the algorithms with different
580 weakness points.

581 The RF was the best all-around algorithm amongst the nine algorithms used in this study,
582 providing the best consistent and robust estimates of the fluxes (similar to XGB) but also being less
583 complicated and performing faster than the XGB. The RF also provided the best results for Fg, where
584 the linear algorithms did not perform well. This superiority of this algorithm over ANNs, MDS, and
585 SVR has been proved by (Kim et al., 2020) for gap-filling of methane, showing that it is worth testing
586 the RF for other towers, and fluxes across the FLUXNET.

587 The ANNs estimated the fluxes better than the linear algorithms, notably for Fc, yet not as
588 robust as the XGB and RF in general. For Fc and Fh, the ANNs provided bias, mainly due to
589 overestimation of minimum values when the window lengths were longer than 30 days. However,
590 since the superiority of the XGB and RF was not considerable, it is difficult at this point to suggest
591 using XGB or RF as better alternatives. That is because ANNs have been checking out for a long time
592 in different locations and considered as one of the most reliable algorithms in the field for more than
593 a decade (Aubinet et al., 2012a; Hagen et al., 2006; Kunwor et al., 2017; Moffat et al., 2007). In other
594 words, the superiority of RF, needs to happen in several future studies to convince the network to
595 suggest RF instead of ANNs, or identify it as another standard method. Furthermore, there are a wide
596 variety of different ANNs algorithms used in the field (Beringer et al., 2016b; Hagen et al., 2006; Isaac
597 et al., 2017; Kunwor et al., 2017; Moffat et al., 2007), and this minor superiority of RF and XGB cannot
598 be generalised without enough additional proves. As such, we suggest other researches to use the RF,
599 especially regarding Fh and Fc alongside the ANNs to find out which one performs better in the

600 challenging scenarios, e.g. when the gaps are long. Another option is to develop ensemble models
601 using since, according to the literature, there is no room to improve the results substantially based on
602 a single algorithm (Moffat et al., 2007). Besides, a model with a higher level of flexibility is required in
603 the field (Hagen et al., 2006; Kunwor et al., 2017; Richardson and Hollinger, 2007). Finally, according
604 to the environmental drivers, The ANNs, like the other ML algorithms, could not show a consistent
605 superiority over the linear algorithms. Therefore, we do not recommend using ML algorithms in such
606 scenarios, except for Fg, for which RF seems to be a better option.

607 The MDS performed close to, yet not as well as the XGB, RF, and ANNS in gap-filling the fluxes.
608 Its performance was close to the SVR, but was more reliable regarding Fe and Fh. It is worth
609 mentioning that this performance was achieved despite the fact that the MDS was using fewer input
610 features. Its performance, however, was comparable with the ML algorithms, particularly when the
611 gap lengths were relatively shorter (smaller than 10 days). As such, we recommend using the MDS
612 when the gaps are not long and/or the available input features are limited, especially considering that
613 the MDS performs significantly faster than the ML algorithms, and is easier to use.

614 The SVR showed consistent inferiority over the other ML algorithms and did not fulfilled our
615 expectations, neither for the meteorological drivers nor for the major fluxes. The only strength of the
616 SVR was that it captured the extreme values better than any other algorithm. However, according to
617 its larger RMSE amounts, the mentioned advantage seems to be achieved suspiciously and might have
618 occurred due to over-fitting. This dubious performance shows the SVR is more vulnerable to the over-
619 fitting issues regarding these types of data. Hence, we suggest the SVR not to be used in any kind of
620 environmental modelling related to the reviewed drivers and fluxes, whatsoever.

621 The CLR, the simplest algorithm used in this research, provided a comparatively acceptable
622 performance in estimating the meteorological drivers, except for Fg. This algorithm, however, could
623 not perform well in assessing the fluxes, especially Fc, mainly because of its inability to capture the
624 extreme values caused by the non-linear nature of Fc. Overall, considering the CLR simplicity,
625 resource-saving and robust performance for drivers, this algorithm seems to be the most suitable way
626 to fill the gaps of meteorological parameters in similar scenarios, where the same ancillary dataset are
627 available.

628 The PD performed slightly better than the CLR, yet it could not fulfil the expectations to show
629 a significant superiority over the other linear algorithms used in the research. This unforeseen weak
630 performance can be explained due to a couple of reasons. First, one of the assumptions of using the
631 PD is that the behaviour of the cross-sections, here towers, is similarly under the similar conditions
632 (the independent variables), and the only thing leads to the difference is the specific characteristics of
633 each individual cross-section. Contrariwise, it seems that the five towers selected in this research
634 violated this assumption due to their absolute different ecosystems. Based on the previous studies in
635 which the PD performed satisfying (Izady et al., 2013, 2016; Mahabbati et al., 2017), (Izady et al., 2016)
636 and (Mahabbati et al., 2017), it appears that a decent level of homogeneity is vital for the PD to perform
637 satisfactorily. As in all previous cases, the ecosystem of the cross-sections had significant similarities,
638 and the distance between them were tens to hundreds of kilometres, not thousands. Therefore, the
639 characteristics of cross-sections, such as radiation, climate, rainfall, etc. had considerable more

640 similarity and homogeneity compared with the towers used in this research. Finally, it is worth
641 mentioning that PD has been commonly used to analyse the time series with a time resolution of
642 weekly or longer, with some exceptional daily-scale cases. In this research, the resolution of data was
643 half-hourly instead, which dramatically increased the computational demands of the algorithm, led
644 to days of processing for a single run. This demand happened because the algorithm creates a dummy
645 variable for each time step and the relevant matrix of variables becomes too large to compute by a
646 regular PC. Considering the expenses of this algorithm, we recommend other researches not to use
647 PD when the time resolution is shorter than daily. Despite the limitation, we still encourage further
648 using of PD whenever there is a decent level of homogeneity amongst the cross-sections and the time
649 resolution is daily or longer (ideally weekly or monthly).

650 The ELN, as a hybrid linear model, did not show any superiority over the CLR, despite its
651 modifications to provide more accurate estimations. Even though ELN performed well in estimating
652 the drivers with slight supremacy in some occasions, e.g. Fld, the CLR is a more proper algorithm to
653 choose for gap-filling the drivers due to its simplicity and less calculation requirement.

654 The FBP was a unique algorithm used in this research, as it did not use any independent
655 variables to estimate the values of drivers and fluxes. The FBP performance was significantly more
656 unsatisfactory than the other algorithms. Therefore FBP cannot be considered as a reliable alternative
657 for current algorithms to fill the gaps, especially the long ones.

658 Given that some of the environmental drivers affect the Fc differently during the day versus
659 night, separating the diurnal and nocturnal datasets to train the algorithms possibly entails an
660 improvement in the outcome. Mainly because of the u^* threshold filtering and other problems
661 associated with the nocturnal period, the portion of diurnal data is generally, by far, outweighs the
662 nocturnal data portion, which potentially leads to a bias in the algorithm. The same challenge has
663 associated with soil moisture estimation, as the behaviour of the system on sunny days is utterly
664 different from its conduct during the rainy periods. Moreover, the system memory and the antecedent
665 condition are undeniable features associated with soil moisture (Ogle et al., 2015). Therefore, using
666 the models that are capable of addressing these considerations are more likely to improve the
667 estimations.

668 5. Conclusions

669 Eight different gap-filling algorithms for estimating 16 meteorological drivers as well as Nine
670 algorithms for the three key ecosystem turbulent fluxes (sensible heat flux (Fh), latent heat flux (Fe),
671 and net carbon flux (Fc)) were investigated and their performance evaluated based on the datasets of
672 five towers in Australia. Overall, three ML algorithms, XGB, RF and ANNs, performed nearly equally
673 well and significantly better than their linear rivals (the CLR, PD, and ELN) in estimating the flux
674 values. However, the linear algorithms performed almost as equally well as the ML algorithms in
675 assessing the meteorological drivers. Amongst these nine algorithms, the RF and XGB showed the
676 highest level of robustness and reliability in estimating the Fc, Fe, and Fh. The PD was expected to
677 perform better than the linear methods and hoped to compete with the ML algorithms in estimating
678 the fluxes, but it failed to do so. The SVR was the only ML algorithm that did not perform at the same

679 level as the rest ML algorithms and was suspected of enduring over-fitting issues, while the MDS
680 performed somewhere in between. Considering the outcomes of the other researches undertaken in
681 the OzFlux Network, e.g. (Cleverly et al., 2013; Isaac et al., 2017), none of the ML algorithms used in
682 this research was proven to provide substantially better flux estimations compared with the standard
683 method (ANNs). Nonetheless, amongst the algorithms tested in this research, the RF showed some
684 potential capabilities as an alternative due to its more consistent performance regarding the long gaps.
685 Eventually, we recommend suggestions below to improve the results for similar prospective
686 researches, as well as the QC and gap-filling procedure of OzFlux Network:

687 1) Since the RF remained more consistent compared to its competitors -including the ANNs-, It is a
688 good idea to use RF alongside the commonly used algorithms in the challenging scenarios, such as
689 long gaps, to figure out whether this superiority can be generalised.

690 2) It appears that, even after three levels of quality control process done by the PyFluxPro platform,
691 the data are still noisy. This noisy data are an essential source of both uncertainty and inaccuracy of
692 the outcome, regardless of the algorithm used to gap-fill the data. As a result, another level of quality
693 control methods, such as Wavelets or Matrix Factorialisation, in addition to the current classical ones
694 used by the PyFluxPro and other similar platforms, can probably improve the data quality and thereby
695 improve the final imputation results.

696 3) For future researches, using recurrent neural networks (RNNs) instead of feedforward neural
697 networks (FFNN) could improve the predictions. That is likely because RNNs help the model to
698 consider temporal dynamic behaviour of time series, as unlike FFNN, wherein the activations flow
699 only from the input layer to the output layer, RNNs also have neuron connections pointing backwards
700 (Géron, 2019). This demand to an algorithm capable of considering time has been mentioned in
701 previous researches as one of the reasons why testing the new algorithms is needed (Richardson and
702 Hollinger, 2007).

703 3) Developing ensemble models using algorithms with different weaknesses and strengths may also
704 enhance the results where a single algorithm shows performance deficiency.

705

706 **6. Data availability**

707 The data were used in this research are available through the following sources: The L3 and L4
708 data are accessible from the OzFlux data portal (<http://data.ozflux.org.au/portal>). Current ACCESS-R
709 and data are available from the BoM OPeNDAP server (<https://www.opendap.org/>). Likewise, the
710 data coming from the BoM AWS are accessible from (<http://www.bom.gov.au/climate/data>). Lastly,
711 the BIOS2 data are accessible from the ECMWF datasets portal
712 (<https://www.ecmwf.int/en/forecasts/datasets>). All data used in this research are available in this
713 repository address: ([https://research-repository.uwa.edu.au/en/datasets/a-comparison-of-gap-filling-
714 algorithms-for-eddy-covariance-fluxes](https://research-repository.uwa.edu.au/en/datasets/a-comparison-of-gap-filling-algorithms-for-eddy-covariance-fluxes)); DOI: [10.26182/5f292ee80a0c0](https://doi.org/10.26182/5f292ee80a0c0).

715

716 *Author contributions.* The ideas for this study originated in discussions with A. Mahabbati, J. Beringer,
717 and M. Leopold. A. Mahabbati carried out the analysis, supported by I. McHugh and P. Isaac. The
718 paper was prepared with contributions from all authors.

719

720 *Competing interests.* The authors declare that they have no conflict of interest.

721

722 *Acknowledgements.* The authors would like to acknowledge Terrestrial Ecosystems Research Network
723 (TERN) (www.tern.gov.au) and the OzFlux Network as a part of TERN for supporting the grants and
724 providing the required data, respectively. A. Mahabbati also personally thanks Prajwal Kalfe, Caroline
725 Johnson and Cacilia Ewenz for their support as regards Python programming, English academic
726 writing and PyFluxPro technical issues.

727

728

729 **References**

730 Allison, P. D.: Multiple Imputation for Missing Data: A Cautionary Tale, *Sociol. Methods Res.*, 28(3), 301–309,
731 doi:10.1177/0049124100028003003, 2000.

732 Altman, D. G. and Bland, J. M.: Missing data, *Br. Med. J.*, 334(7590), 424, doi:10.1136/bmj.38977.682025.2C, 2007.

733 Aubinet, M., Grelle, A., Ibrom, A., Rannik, Ü., Moncrieff, J., Foken, T., Kowalski, A. S., Martin, P. H., Berbigier, P., Bernhofer, C.,
734 Clement, R., Elbers, J., Granier, A., Grünwald, T., Morgenstern, K., Pilegaard, K., Rebmann, C., Snijders, W., Valentini, R. and
735 Vesala, T.: Estimates of the Annual Net Carbon and Water Exchange of Forests: The EUROFLUX Methodology, *Adv. Ecol. Res.*, 30,
736 113–175, doi:10.1016/S0065-2504(08)60018-5, 1999.

737 Aubinet, M., Vesala, T. and Papale, D.: *Eddy Covariance: A Practical Guide to Measurement and Data Analysis.*, 2012a.

738 Aubinet, M., Vesala, T. and Papale, D.: *Eddy Covariance.*, 2012b.

739 Baldocchi, D., Falge, E., Gu, L., Olson, R., Hollinger, D., Running, S., Anthoni, P., Bernhofer, C., Davis, K., Evans, R., Fuentes, J.,
740 Goldstein, A., Katul, G., Law, B., Lee, X., Malhi, Y., Meyers, T., Munger, W., Oechel, W., Paw, U. K. T., Pilegaard, K., Schmid, H. P.,
741 Valentini, R., Verma, S., Vesala, T., Wilson, K. and Wofsy, S.: FLUXNET: A New Tool to Study the Temporal and Spatial Variability
742 of Ecosystem-Scale Carbon Dioxide, Water Vapor, and Energy Flux Densities, *Bull. Am. Meteorol. Soc.*, 82(11), 2415–2434,
743 doi:10.1175/1520-0477(2001)082<2415:FANTTS>2.3.CO;2, 2001.

744 Baltagi, B.: *Econometric analysis of panel data*, [online] Available from: [http://www.sidalc.net/cgi-](http://www.sidalc.net/cgi-bin/wxis.exe/?IsisScript=book2.xis&method=post&formato=2&cantidad=1&expresion=mfn=001143)
745 [bin/wxis.exe/?IsisScript=book2.xis&method=post&formato=2&cantidad=1&expresion=mfn=001143](http://www.sidalc.net/cgi-bin/wxis.exe/?IsisScript=book2.xis&method=post&formato=2&cantidad=1&expresion=mfn=001143) (Accessed 13 March 2018), 1995.

746 Barr, A. G., Black, T. A., Hogg, E. H., Kljun, N., Morgenstern, K. and Nesic, Z.: Inter-annual variability in the leaf area index of a
747 boreal aspen-hazelnut forest in relation to net ecosystem production, *Agric. For. Meteorol.*, 126(3–4), 237–255,
748 doi:10.1016/J.AGRFORMET.2004.06.011, 2004.

749 Barr, A. G., Richardson, A. D., Hollinger, D. Y., Papale, D., Arain, M. A., Bohrer, G., Dragoni, D., Fischer, M. L., Gu, L.,
750 Law, B. E., Margolis, H. A., Mccaughey, J. H., Munger, J. W., Oechel, W. and Schaeffer, K.: Use of change-point detection for friction-
751 velocity threshold evaluation in eddy-covariance studies, *Agric. For. Meteorol.*, 171–172, 31–45, doi:10.1016/j.agrformet.2012.11.023,
752 2013.

753 Bennett, N. D., Croke, B. F. W., Guariso, G., Guillaume, J. H. A., Hamilton, S. H., Jakeman, A. J., Marsili-Libelli, S., Newham, L. T.
754 H., Norton, J. P., Perrin, C., Pierce, S. A., Robson, B., Seppelt, R., Voinov, A. A., Fath, B. D. and Andreassian, V.: Characterising
755 performance of environmental models, *Environ. Model. Softw.*, 40, 1–20, doi:10.1016/j.envsoft.2012.09.011, 2013.

756 Beringer, J., Hutley, L. B., McHugh, I., Arndt, S. K., Campbell, D., Cleugh, H. A., Cleverly, J., De Dios, V. R., Eamus, D., Evans, B.,
757 Ewenz, C., Grace, P., Griebel, A., Haverd, V., Hinko-Najera, N., Huete, A., Isaac, P., Kanniah, K., Leuning, R., Liddell, M. J.,
758 MacFarlane, C., Meyer, W., Moore, C., Pendall, E., Phillips, A., Phillips, R. L., Prober, S. M., Restrepo-Coupe, N., Rutledge, S.,
759 Schroder, I., Silberstein, R., Southall, P., Sun Yee, M., Tapper, N. J., Van Gorsel, E., Vote, C., Walker, J. and Wardlaw, T.: An
760 introduction to the Australian and New Zealand flux tower network - OzFlux, *Biogeosciences*, 13(21), 5895–5916, doi:10.5194/bg-13-

- 761 5895-2016, 2016a.
- 762 Beringer, J., McHugh, I. and Kljun, N.: Dynamic INtegrated Gap filling and partitioning for Ozflux (DINGO), Biogeosciences
763 Discuss., OzFlux spe(In prep), 1457–1460, doi:doi:10.5194/bg-2016-188, 2016b.
- 764 Beringer, J., McHugh, I., Hutley, L. B., Isaac, P. and Kljun, N.: Technical note: Dynamic INtegrated Gap-filling and partitioning for
765 OzFlux (DINGO), Biogeosciences, 14(6), 1457–1460, doi:10.5194/bg-14-1457-2017, 2017.
- 766 Burba, G. and Anderson, D.: A brief practical guide to eddy covariance flux measurements: principles and workflow examples for
767 scientific and industrial applications. [online] Available from:
768 https://books.google.com/books?hl=en&lr=&id=mCsI1_8GdriC&oi=fnd&pg=PA6&dq=A+Brief+Practical+Guide+to+Eddy+Covariance+Flux+Measurements&ots=TKTg25Yq5X&sig=eBYc819N7Jh3gNhJnfEL1e40eM (Accessed 11 February 2020), 2010.
769
- 770 Chen, T. and Guestrin, C.: XGBoost: A scalable tree boosting system, Proc. ACM SIGKDD Int. Conf. Knowl. Discov. Data Min., 13-
771 17-Aug, 785–794, doi:10.1145/2939672.2939785, 2016.
- 772 Cleverly, J., Boulain, N., Villalobos-Vega, R., Grant, N., Faux, R., Wood, C., Cook, P. G., Yu, Q., Leigh, A. and Eamus, D.: Dynamics
773 of component carbon fluxes in a semi-arid *Acacia* woodland, central Australia, J. Geophys. Res. Biogeosciences, 118(3), 1168–1185,
774 doi:10.1002/jgrg.20101, 2013.
- 775 Devore, J. L.: Probability and Statistics for Engineering and the Sciences., Biometrics, 47(4), 1638, doi:10.2307/2532427, 1991.
- 776 Dragoni, D., Schmid, H. P., Grimmond, C. S. B. and Loescher, H. W.: Uncertainty of annual net ecosystem productivity estimated
777 using eddy covariance flux measurements, J. Geophys. Res., 112(D17), D17102, doi:10.1029/2006JD008149, 2007.
- 778 Dreyfus, S. E.: Artificial neural networks, back propagation, and the kelley-bryson gradient procedure, J. Guid. Control. Dyn., 13(5),
779 926–928, doi:10.2514/3.25422, 1990.
- 780 Drucker, H., Surges, C. J. C., Kaufman, L., Smola, A. and Vapnik, V.: Support vector regression machines, in Advances in Neural
781 Information Processing Systems, vol. 1, pp. 155–161., 1997.
- 782 Falge, E., Baldocchi, D., Olson, R., Anthoni, P., Aubinet, M., Bernhofer, C., Burba, G., Ceulemans, R., Clement, R., Dolman, H.,
783 Granier, A., Gross, P., Grünwald, T., Hollinger, D., Jensen, N. O., Katul, G., Keronen, P., Kowalski, A., Lai, C. T., Law, B. E., Meyers,
784 T., Moncrieff, J., Moors, E., Munger, J. W., Pilegaard, K., Rannik, Ü., Rebmann, C., Suyker, A., Tenhunen, J., Tu, K., Verma, S.,
785 Vesala, T., Wilson, K. and Wofsy, S.: Gap filling strategies for defensible annual sums of net ecosystem exchange, Agric. For.
786 Meteorol., 107(1), 43–69, doi:10.1016/S0168-1923(00)00225-2, 2001.
- 787 Farley, B. G. and Clark, W. A.: Simulation of self-organizing systems by digital computer, IRE Prof. Gr. Inf. Theory, 4(4), 76–84,
788 doi:10.1109/TIT.1954.1057468, 1954.
- 789 Freedman, D. A.: Statistical Models: Theory and Practice. Cambridge University Press - 2nd edition. [online] Available from:
790 <https://www.cambridge.org/au/academic/subjects/statistics-probability/statistical-theory-and-methods/statistical-models-theory-and-practice-2nd-edition?format=PB> (Accessed 21 March 2020), 2009.
791
- 792 Friedman, J. H.: Stochastic gradient boosting, Comput. Stat. Data Anal., 38(4), 367–378, doi:10.1016/S0167-9473(01)00065-2, 2002.
- 793 Gani, A., Mohammadi, K., Shamshirband, S., Altameem, T. A., Petković, D. and Ch, S.: A combined method to estimate wind speed
794 distribution based on integrating the support vector machine with firefly algorithm, Environ. Prog. Sustain. Energy, 35(3), 867–875,
795 doi:10.1002/ep.12262, 2016.
- 796 Géron, A.: Hands-on machine learning with Scikit-Learn and TensorFlow: concepts, tools, and techniques to build intelligent
797 systems. [online] Available from:
798 <https://books.google.com.au/books?hl=en&lr=&id=HHetDwAAQBAJ&oi=fnd&pg=PP1&dq=hands-on+machine+learning+with+&ots=0KvfZqlgOo&sig=5tH2IHRsUaTMTy6CfQ6lw3UDKa4> (Accessed 7 February 2020), 2019.
799
- 800 Hagen, S. C., Braswell, B. H., Linder, E., Frohling, S., Richardson, A. D. and Hollinger, D. Y.: Statistical uncertainty of eddy flux -
801 Based estimates of gross ecosystem carbon exchange at Howland Forest, Maine, J. Geophys. Res. Atmos., 111(8), 1–12,
802 doi:10.1029/2005JD006154, 2006.
- 803 Harrell, F. E.: Regression Modeling Strategies: With Applications to Linear Models, Logistic, in books.google.nl. [online] Available
804 from:
805 <https://books.google.com.au/books?hl=en&lr=&id=94RgCgAAQBAJ&oi=fnd&pg=PR7&dq=regression+modeling+strategies+frank+h>
806 [arrell&ots=ZA4tRsaS1r&sig=mikE1s9G4IXzqZKEie-iVA9GTV0&redir_esc=y#v=onepage&q=regression modeling strategies frank](https://books.google.com.au/books?hl=en&lr=&id=94RgCgAAQBAJ&oi=fnd&pg=PR7&dq=regression+modeling+strategies+frank+h)
807 [harrell&f=false](https://books.google.com.au/books?hl=en&lr=&id=94RgCgAAQBAJ&oi=fnd&pg=PR7&dq=regression+modeling+strategies+frank+h) (Accessed 11 February 2020), 2014.

- 808 Harvey, A. C. and Peters, S.: Estimation procedures for structural time series models, *J. Forecast.*, 9(2), 89–108,
809 doi:10.1002/for.3980090203, 1990.
- 810 Haverd, V., Briggs, P., Trudinger, C., Nieradzik, L. and Canadell, P.: BIOS2 – Frontier Modelling of the Australian Carbon and
811 Water Cycles, 2015.
- 812 Ho, T. K.: Random decision forests, *Proc. Int. Conf. Doc. Anal. Recognition, ICDAR*, 1, 278–282, doi:10.1109/ICDAR.1995.598994,
813 1995.
- 814 Ho, T. K.: 00709601.Pdf, , 20(8), 832–844, 1998.
- 815 Hollinger, D. Y., Goltz, S. M., Davidson, E. A., Lee, J. T., Tu, K. and Valentine, H. T.: Seasonal patterns and environmental control of
816 carbon dioxide and water vapour exchange in an ecotonal boreal forest, *Glob. Chang. Biol.*, 5(8), 891–902, doi:10.1046/j.1365-
817 2486.1999.00281.x, 1999.
- 818 Hsiao, C., Hashem Pesaran, M. and Kamil Tahmiscioglu, A.: Maximum likelihood estimation of fixed effects dynamic panel data
819 models covering short time periods, *J. Econom.*, 109(1), 107–150, doi:10.1016/S0304-4076(01)00143-9, 2002.
- 820 Hui, D., Wan, S., Su, B., Katul, G., Monson, R. and Luo, Y.: Gap-filling missing data in eddy covariance measurements using
821 multiple imputation (MI) for annual estimations, *Agric. For. Meteorol.*, 121(1–2), 93–111, doi:10.1016/S0168-1923(03)00158-8, 2004.
- 822 Hutley, L. B., Leuning, R., Beringer, J. and Cleugh, H. a: The utility of the eddy covariance technique as a tool in carbon accounting:
823 tropical savanna as a case study, *Aust. J. Bot.*, 53, 663–675, 2005.
- 824 Isaac, P., Cleverly, J., McHugh, I., Van Gorsel, E., Ewenz, C. and Beringer, J.: OzFlux data: Network integration from collection to
825 curation, *Biogeosciences*, 14(12), 2903–2928, doi:10.5194/bg-14-2903-2017, 2017.
- 826 Izady, A., Davary, K., Alizadeh, A., Moghaddam Nia, A., Ziaei, A. N. and Hashemina, S. M.: Application of NN-ARX Model to
827 Predict Groundwater Levels in the Neishaboer Plain, Iran, *Water Resour. Manag.*, 27(14), 4773–4794, doi:10.1007/s11269-013-0432-y,
828 2013.
- 829 Izady, A., Abdalla, O. and Mahabbati, A.: Dynamic panel-data-based groundwater level prediction and decomposition in an arid
830 hardrock–alluvium aquifer, *Environ. Earth Sci.*, 75(18), 1–13, doi:10.1007/s12665-016-6059-6, 2016.
- 831 Jerome H. Friedman: Greedy Function Approximation: A Gradient Boosting Machine on JSTOR, *Ann. Stat.*, 29, 1189–1232 [online]
832 Available from: https://www.jstor.org/stable/2699986?seq=1#metadata_info_tab_contents (Accessed 27 August 2019), 2001.
- 833 Kang, H.: The prevention and handling of the missing data, *Korean J. Anesthesiol.*, 64(5), 402–406, doi:10.4097/kjae.2013.64.5.402,
834 2013.
- 835 Kim, Y., Johnson, M. S., Knox, S. H., Black, T. A., Dalmagro, H. J., Kang, M., Kim, J. and Baldocchi, D.: Gap-filling approaches for
836 eddy covariance methane fluxes: A comparison of three machine learning algorithms and a traditional method with principal
837 component analysis, *Glob. Chang. Biol.*, 26(3), 1499–1518, doi:10.1111/gcb.14845, 2020.
- 838 Kock, N. and Gaskins, L.: Simpson’s paradox, moderation and the emergence of quadratic relationships in path models: an
839 information systems illustration, *Int. J. Appl. Nonlinear Sci.*, 2(3), 200, doi:10.1504/ijans.2016.077025, 2016.
- 840 Kunwor, S., Starr, G., Loescher, H. W. and Staudhammer, C. L.: Preserving the variance in imputed eddy-covariance measurements:
841 Alternative methods for defensible gap filling, *Agric. For. Meteorol.*, 232, 635–649, doi:10.1016/j.agrformet.2016.10.018, 2017.
- 842 Law, B. E., Falge, E., Gu, L., Baldocchi, D. D., Bakwin, P., Berbigier, P., Davis, K., Dolman, A. J., Falk, M., Fuentes, J. D., Goldstein,
843 A., Granier, A., Grelle, A., Hollinger, D., Janssens, I. A., Jarvis, P., Jensen, N. O., Katul, G., Mahli, Y., Matteucci, G., Meyers, T.,
844 Monson, R., Munger, W., Oechel, W., Olson, R., Pilegaard, K., Paw U H, K. T., Thorgeirsson, H., Valentini, R., Verma, S., Vesala, T.,
845 Wilson, K. and Wofsy, S.: Jourassess2, *Agric. For. Meteorol.*, 113(113), 97–120, 2002.
- 846 Lee, X., Fuentes, J. D., Staebler, R. M. and Neumann, H. H.: Long-term observation of the atmospheric exchange of CO₂ with a
847 temperate deciduous forest in southern Ontario, Canada, *J. Geophys. Res. Atmos.*, 104(D13), 15975–15984,
848 doi:10.1029/1999JD900227, 1999.
- 849 Little, R. J. A.: *Statistical analysis with missing data*, 2nd ed., edited by D. B. Rubin, Wiley, Hoboken, N.J., 2002.
- 850 Mahabbati, A., Izady, A., Mousavi Baygi, M., Davary, K. and Hashemina, S. M.: Daily soil temperature modeling using ‘panel-data’
851 concept, *J. Appl. Stat.*, 44(8), 1385–1401, doi:10.1080/02664763.2016.1214240, 2017.
- 852 Menzer, O., Moffat, A. M., Meiring, W., Lasslop, G., Schukat-Talamazzini, E. G. and Reichstein, M.: Random errors in carbon and

- 853 water vapor fluxes assessed with Gaussian Processes, *Agric. For. Meteorol.*, 178–179, 161–172, doi:10.1016/j.agrformet.2013.04.024,
854 2013.
- 855 Moffat, A. M., Papale, D., Reichstein, M., Hollinger, D. Y., Richardson, A. D., Barr, A. G., Beckstein, C., Braswell, B. H., Churkina, G.,
856 Desai, A. R., Falge, E., Gove, J. H., Heimann, M., Hui, D., Jarvis, A. J., Kattge, J., Noormets, A. and Stauch, V. J.: Comprehensive
857 comparison of gap-filling techniques for eddy covariance net carbon fluxes, *Agric. For. Meteorol.*, 147(3–4), 209–232,
858 doi:10.1016/j.agrformet.2007.08.011, 2007.
- 859 Molenberghs, G., Fitzmaurice, G., Kenward, M. G., Tsiatis, A., Verbeke, G., Fitzmaurice, G., Kenward, M. G., Tsiatis, A. and
860 Verbeke, G.: *Handbook of Missing Data Methodology*, Chapman and Hall/CRC., 2014.
- 861 Ogle, K., Barber, J. J., Barron-Gafford, G. A., Bentley, L. P., Young, J. M., Huxman, T. E., Loik, M. E. and Tissue, D. T.: Quantifying
862 ecological memory in plant and ecosystem processes, *Ecol. Lett.*, 18(3), 221–235, doi:10.1111/ele.12399, 2015.
- 863 Papale, D. and Valentini, R.: A new assessment of European forests carbon exchanges by eddy fluxes and artificial neural network
864 spatialization, *Glob. Chang. Biol.*, 9(4), 525–535, doi:10.1046/j.1365-2486.2003.00609.x, 2003.
- 865 Pilegaard, K., Hummelshøj, P., Jensen, N. O. and Chen, Z.: Two years of continuous CO₂ eddy-flux measurements over a Danish
866 beech forest, *Agric. For. Meteorol.*, 107(1), 29–41, doi:10.1016/S0168-1923(00)00227-6, 2001.
- 867 Reichle, R. H., Koster, R. D., Dong, J. and Berg, A. A.: Global soil moisture from satellite observations, land surface models, and
868 ground data: Implications for data assimilation, *J. Hydrometeorol.*, 5(3), 430–442, doi:10.1175/1525-
869 7541(2004)005<0430:GSMFSC>2.0.CO;2, 2004.
- 870 Reichstein, M., Falge, E., Baldocchi, D., Papale, D., Aubinet, M., Berbigier, P., Bernhofer, C., Buchmann, N., Gilmanov, T., Granier,
871 A., Grünwald, T., Havránková, K., Ilvesniemi, H., Janous, D., Knohl, A., Laurila, T., Lohila, A., Loustau, D., Matteucci, G., Meyers,
872 T., Miglietta, F., Ourcival, J. M., Pumpanen, J., Rambal, S., Rotenberg, E., Sanz, M., Tenhunen, J., Seufert, G., Vaccari, F., Vesala, T.,
873 Yakir, D. and Valentini, R.: On the separation of net ecosystem exchange into assimilation and ecosystem respiration: Review and
874 improved algorithm, *Glob. Chang. Biol.*, 11(9), 1424–1439, doi:10.1111/j.1365-2486.2005.001002.x, 2005.
- 875 Richardson, A. D. and Hollinger, D. Y.: A method to estimate the additional uncertainty in gap-filled NEE resulting from long gaps
876 in the CO₂ flux record, *Agric. For. Meteorol.*, 147(3–4), 199–208, doi:10.1016/j.agrformet.2007.06.004, 2007.
- 877 Richardson, A. D., Braswell, B. H., Hollinger, D. Y., Burman, P., Davidson, E. A., Evans, R. S., Flanagan, L. B., Munger, J. W., Savage,
878 K., Urbanski, S. P. and Wofsy, S. C.: Comparing simple respiration models for eddy flux and dynamic chamber data, *Agric. For.*
879 *Meteorol.*, 141(2–4), 219–234, doi:10.1016/J.AGRFORMET.2006.10.010, 2006.
- 880 Richardson, A. D., Aubinet, M., Barr, A. G., Hollinger, D. Y., Ibrom, A., Lasslop, G. and Reichstein, M.: Uncertainty Quantification,
881 in *Eddy Covariance*, pp. 173–209., 2012.
- 882 Sahoo, A. K., Dirmeyer, P. A., Houser, P. R. and Kafatos, M.: A study of land surface processes using land surface models over the
883 Little River Experimental Watershed, Georgia, *J. Geophys. Res. Atmos.*, 113(20), doi:10.1029/2007JD009671, 2008.
- 884 Scanlon, T. M. and Kustas, W. P.: Partitioning carbon dioxide and water vapor fluxes using correlation analysis, *Agric. For.*
885 *Meteorol.*, 150(1), 89–99, doi:10.1016/j.agrformet.2009.09.005, 2010.
- 886 Scanlon, T. M. and Sahu, P.: On the correlation structure of water vapor and carbon dioxide in the atmospheric surface layer: A
887 basis for flux partitioning, *Water Resour. Res.*, 44(10), doi:10.1029/2008WR006932, 2008.
- 888 Staebler, M.: Long-term observation of the atmospheric exchange of CO₂ with a temperate deciduous forest in southern Ontario ,
889 Canada ecosystem (net ecosystem production turbulence is turbulent, *Data Process.*, 104, 975–984, 1999.
- 890 Tannenbaum, C. E.: The empirical nature and statistical treatment of missing data., *Diss. Abstr. Int. Sect. A Humanit. Soc. Sci.*, 70(10-
891 A), 3825 [online] Available from: http://gateway.proquest.com/openurl?url_ver=Z39.88-2004&rft_val_fmt=info:ofi/fmt:kev:mtx:dissertation&res_dat=xri:pqdiss&rft_dat=xri:pqdiss:3381876%5Cnhttp://ovidsp.ovid.com/ovidweb.cgi?T=JS&PAGE=reference&D=psyc7&NEWS=N&AN=2010-99071-044, 2010.
- 894 Taylor, S. J. and Letham, B.: *Business Time Series Forecasting at Scale*, doi:10.7287/peerj.preprints.3190v2, 2017.
- 895 Taylor, S. J. and Letham, B.: *Forecasting at Scale*, *Am. Stat.*, 72(1), 37–45, doi:10.1080/00031305.2017.1380080, 2018.
- 896 Tenhunen, J. D., Valentini, R., Köstner, B., Zimmermann, R. and Granier, A.: Variation in forest gas exchange at landscape to
897 continental scales, *Ann. des Sci. For.*, 55(1–2), 1–11, doi:10.1051/forest:19980101, 1998.

- 898 Wooldridge, J. M.: *Econometric Analysis of Cross Section and Panel Data*, 2008.
- 899 Ye, J., Chow, J.-H., Chen, J. and Zheng, Z.: Stochastic gradient boosted distributed decision trees, in *Proceeding of the 18th ACM*
900 *conference on Information and knowledge management - CIKM '09*, p. 2061, ACM Press, New York, New York, USA., 2009.
- 901 Zhao, X. and Huang, Y.: A comparison of three gap filling techniques for eddy covariance net carbon fluxes in short vegetation
902 ecosystems, *Adv. Meteorol.*, 2015, 1–12, doi:10.1155/2015/260580, 2015.
- 903 Zou, H. and Hastie, T.: Regularization and variable selection via the elastic net. [online] Available from:
904 [https://citeseerx.ist.psu.edu/viewdoc/download;jsessionid=22250F01CC77D55C54B6BAFF4512C9E3?doi=10.1.1.124.4696&rep=rep1&](https://citeseerx.ist.psu.edu/viewdoc/download;jsessionid=22250F01CC77D55C54B6BAFF4512C9E3?doi=10.1.1.124.4696&rep=rep1&type=pdf)
905 [type=pdf](https://citeseerx.ist.psu.edu/viewdoc/download;jsessionid=22250F01CC77D55C54B6BAFF4512C9E3?doi=10.1.1.124.4696&rep=rep1&type=pdf) (Accessed 28 August 2019), 2005.